

A “SEMI-ANALOG” MONTE CARLO METHOD FOR GREY RADIATIVE TRANSFER PROBLEMS

Cory Ahrens and Edward W. Larsen

Department of Nuclear Engineering and Radiological Sciences

University of Michigan

Ann Arbor, MI 48109-2104 USA

cahrens@umich.edu, edlarsen@umich.edu

Keywords: thermal radiative transfer, Monte Carlo

ABSTRACT

Time-dependent thermal radiative transfer differs from time-dependent neutron transport because of the *absorption* and *emission* processes in radiative transfer. The “Implicit Monte Carlo” (IMC) simulation of radiative transfer approximates absorption and emission, causing temporal and spatial truncation errors. In this paper we develop a new “Semi-Analog Monte Carlo” (SMC) method for grey (frequency-independent) thermal radiative transfer. The SMC method avoids all of the IMC approximations except for those due to nonlinearities. For linear grey radiative transfer, the SMC method is *analog* – it faithfully models all the radiative transfer physics. For nonlinear grey radiative transfer, the SMC method has (linearization) truncation errors and is not analog. (The grey IMC method always has truncation errors and is never analog.) In this paper we describe the grey SMC method and compare it, analytically and numerically, to grey IMC.

1. INTRODUCTION

In radiative transfer processes, photons are born and then stream to random collision sites, where they are randomly scattered or *absorbed* by the material. If a photon scatters, it immediately streams on toward its next collision site. If a photon is absorbed, its energy remains at the absorption site until a later random time, when it is *emitted* in the form of one or more new photons (Pomraning, 1973), (Mihalas, 1984).

This time-dependent radiative transfer process can be simulated by the “Implicit Monte Carlo” (IMC) method of Fleck and Cummings (Fleck, 1971). Although designed for Monte Carlo simulations, the IMC method has been adapted for deterministic simulations (Alcouffe, 1985). The Monte Carlo IMC method treats photon scattering and streaming correctly, but it approximates photon absorption and emission. This yields a time-dependent transport equation with *pseudo*-scattering, which governs the IMC process during each time step. The Monte Carlo simulation of this approximate transport equation is the essence of the IMC scheme. However, the discretization errors in IMC can cause unphysical behavior for large time steps (Larsen, 1987).

This paper, an expanded version of a recent ANS abstract (Ahrens, 2000), presents a new Monte Carlo algorithm for grey (frequency-independent) radiative transfer problems.

For linear problems, our new method is *analog* – it faithfully models all the radiative transfer physics. The only errors in simulations of such problems are statistical. For nonlinear problems, the new method has (linearization) truncation errors and hence is not analog. (The IMC method always has truncation errors and is never analog.) The particular nonlinear structure of the radiative transfer equations is *semilinear* (Chester, 1971). We describe the Monte Carlo method proposed in this paper as *Semi-Analog Monte Carlo* (SMC), in recognition of this mathematical structure, and to emphasize that for linear problems, the new method is truly analog.

The SMC method is similar to a Monte Carlo method proposed previously by Carter and Forest (Carter, 1973), (Martin, 2001). In both the SMC and Carter-Forest (CF) methods, the simulation of linear radiative transfer problems is identical *within a timestep*. However, the CF method introduces approximations – in order to reduce storage – at the end of each timestep. These approximations render the CF scheme nonanalog for linear problems.

The remainder of this paper is organized as follows. In Section 2 we develop the grey equations of radiative transfer. In Section 3 we sketch a derivation of the IMC method that enables a direct comparison with the SMC method. In Section 4 we develop the SMC method, and in Section 5 we numerically compare the IMC and SMC solutions for a planar geometry problem solved by Su and Olson (Su, 1997). We conclude with a discussion in Section 6.

2. NONLINEAR AND LINEAR GREY RADIATIVE TRANSFER

We denote the familiar space, direction-of-flight, frequency, and time variables as $\underline{r} = (x, y, z)$, $\underline{\Omega} = (\Omega_x, \Omega_y, \Omega_z)$ [$|\underline{\Omega}| = 1$], ν , and t . Then the equations of thermal radiative transfer without scattering are (Pomraning, 1973), (Mihalas, 1984):

$$\frac{1}{c} \frac{\partial I}{\partial t} + \underline{\Omega} \cdot \nabla I = \sigma(B - I) + \frac{Q}{4\pi} , \quad (1)$$

$$\frac{\partial U_m}{\partial t} = \int_0^\infty \int_{4\pi} \sigma(I - B) d\Omega' d\nu' . \quad (2)$$

Here c is the speed of light; the functions

$$\sigma(\underline{r}, \nu, T) = \text{opacity} , \quad (3)$$

$$U_m(\underline{r}, T) = \text{material energy density} , \quad (4)$$

$$Q(\underline{r}, \nu, t) = \text{isotropic photon source} , \quad (5)$$

$$B(\nu, T) = \frac{2h}{c^2} \frac{\nu^3}{e^{h\nu/kT} - 1} = \text{Planck function} , \quad (6)$$

(with h = Planck's constant and k = Boltzmann's constant) are specified; and the functions

$$I(\underline{r}, \underline{\Omega}, \nu, t) = \text{specific intensity} , \quad (7)$$

$$T(\underline{r}, t) = \text{material temperature} , \quad (8)$$

are to be determined.

Eqs. (1) and (2) are linear in I , but nonlinear in T . They hold in a 3-D spatial region R . Initial conditions specifying I and T must be prescribed at an initial time for all points in

R , and values of I must be specified on the outer boundary of R for all directions $\underline{\Omega}$ pointing into R and all times later than the initial time (Pomraning, 1973). We permit σ and U_m to depend on \underline{r} independently of T , to allow problems with different material regions. [For example, a certain subregion of R could be a void, in which $\sigma(\underline{r}, \nu, T) = 0$.] The Planck function satisfies

$$\int_0^\infty B(\nu, T) d\nu = \frac{acT^4}{4\pi} , \quad (9)$$

$$\left[a = \frac{8\pi^5 k^4}{15h^3 c^3} = \text{radiation constant} \right] , \quad (10)$$

and we define

$$c_\nu(\underline{r}, T) = \frac{\partial U_m}{\partial T}(\underline{r}, T) = \text{heat capacity} \quad (> 0) . \quad (11)$$

For a perfect gas, c_ν is independent of T (Fleck, 1971).

For the special case of a frequency-independent opacity:

$$\sigma(\underline{r}, \nu, T) = \sigma(\underline{r}, T) = \sigma[\underline{r}, T(\underline{r}, t)] , \quad (12)$$

Eqs. (1) and (2) can be simplified to equations for $T(\underline{r}, t)$ and

$$\psi(\underline{r}, \underline{\Omega}, t) = \int_0^\infty I(\underline{r}, \underline{\Omega}, \nu, t) d\nu = \text{frequency - integrated ("grey")} \text{ intensity} . \quad (13)$$

To accomplish this, we integrate Eq. (1) over ν . Using that result and Eq. (2), together with Eqs. (9), (12), (13), and:

$$q(\underline{r}, t) = \int_0^\infty Q(\underline{r}, \nu, t) d\nu = \text{frequency - integrated source} , \quad (14)$$

$$U_r(\underline{r}, t) = aT^4(\underline{r}, t) = \text{equilibrium radiation energy density} , \quad (15)$$

we obtain the *grey radiative transfer* equations, which are independent of ν :

$$\frac{1}{c} \frac{\partial \psi}{\partial t} + \underline{\Omega} \cdot \underline{\nabla} \psi = \sigma \left(\frac{cU_r}{4\pi} - \psi \right) + \frac{q}{4\pi} , \quad (16)$$

$$\frac{\partial U_m}{\partial t} = \sigma \left(\int_{4\pi} \psi d\Omega' - cU_r \right) . \quad (17)$$

These equations are the subject of the remainder of this paper. Integrating Eq. (16) over $\underline{\Omega}$ and adding the result to Eq. (17), we obtain the *energy-conservation* equation:

$$\frac{\partial}{\partial t} \left(\frac{1}{c} \int_{4\pi} \psi d\Omega + U_m \right) + \underline{\nabla} \cdot \left(\int_{4\pi} \underline{\Omega} \psi d\Omega \right) = q , \quad (18)$$

which is satisfied in the IMC and SMC methods. In general, the opacity σ is temperature-dependent, i.e. it depends on the solution. Also, $U_m = U_m(T)$ and $U_r = aT^4$, so U_m and

U_r are related nonlinearly. For these reasons, Eqs. (15)-(17) are linear in I but are generally nonlinear in T . [Specifically, they are a system of *semilinear* equations in ψ and U_m (Chester, 1971).] However, in the special case (Su, 1997)

$$\sigma(\underline{r}, T) = \sigma(\underline{r}) \quad (\text{independent of } T) \quad , \quad (19)$$

$$U_m(\underline{r}, T) = \frac{U_r(T)}{\eta(\underline{r})} = \frac{aT^4}{\eta(\underline{r})} \quad , \quad (20)$$

$$\left[c_v(\underline{r}, T) = \frac{4aT^3}{\eta(\underline{r})} \right] \quad , \quad (21)$$

where $\eta(\underline{r})$ is a specified dimensionless function, Eqs. (16) and (17) become

$$\frac{1}{c} \frac{\partial \psi}{\partial t} + \underline{\Omega} \cdot \underline{\nabla} \psi = \sigma \left(\frac{c\eta U_m}{4\pi} - \psi \right) + \frac{q}{4\pi} \quad , \quad (22)$$

$$\frac{\partial U_m}{\partial t} = \sigma \left(\int_{4\pi} \psi d\Omega' - c\eta U_m \right) \quad , \quad (23)$$

and these equations are linear in ψ and U_m .

Before proceeding, we briefly discuss some common features of the IMC and SMC methods:

1. Both methods approximate the values of $\sigma(\underline{r}, T)$ during a time step $t_n \leq t < t_{n+1}$ by using the known temperature at the beginning of the time step. Thus, if

$$\sigma_n = \sigma_n(\underline{r}) = \sigma[\underline{r}, T(\underline{r}, t_n)] \quad , \quad (24)$$

then the IMC and SMC methods employ the following approximation of Eqs. (16) and (17):

$$\frac{1}{c} \frac{\partial \psi}{\partial t} + \underline{\Omega} \cdot \underline{\nabla} \psi = \sigma_n \left(\frac{cU_r}{4\pi} - \psi \right) + \frac{q}{4\pi} \quad , \quad (25)$$

$$\frac{\partial U_m}{\partial t} = \sigma_n \left(\int_{4\pi} \psi d\Omega' - cU_r \right) \quad , \quad (26)$$

for $t_n \leq t < t_{n+1}$. This eliminates one of the potential nonlinearities in the grey equations. The energy balance equation (18) does not contain σ , so this approximation conserves energy.

2. The energy balance equation does not contain U_r , so replacing Eq. (15) for U_r by a linear approximation also conserves energy. This eliminates the second potential nonlinearity in the grey equations.
3. The IMC and SMC methods are *linearizations* of Eqs. (25) and (26). However, the SMC method linearizes in such a way that if the equations were linear to begin with, then no change would occur.

3. Implicit Monte Carlo (IMC)

The IMC method is based on the observation that if Eq. (15) is approximated by expressing U_r in terms of ψ (rather than T), Eqs. (25) and (26) would be coupled in a simpler lower-triangular manner. That is, Eq. (25) would depend only on ψ , so it could be solved during a time step independently of Eq. (26). Afterward, the results for ψ could be introduced into the right side of Eq. (26), to update U_m and T .

To obtain such an approximate relationship between $U_r(\underline{r}, t)$ and $\psi(\underline{r}, \underline{\Omega}, t)$, we introduce

$$\frac{\partial U_m}{\partial t} = \frac{\partial U_m}{\partial T} \frac{dT}{dU_r} \frac{\partial U_r}{\partial t} = \frac{c_v(T)}{4aT^3} \frac{\partial U_r}{\partial t} \approx \frac{c_v(T_n)}{4aT_n^3} \frac{\partial U_r}{\partial t} \equiv \frac{1}{\beta_n} \frac{\partial U_r}{\partial t} \quad (27)$$

into Eq. (26), yielding:

$$\frac{1}{\beta_n} \frac{\partial U_r}{\partial t} = \sigma_n \left(\int_{4\pi} \psi d\Omega - cU_r \right) . \quad (28)$$

Integrating over $t_n \leq t' \leq t$, using $U_r(\underline{r}, t_n) = aT_n^4(\underline{r}, t_n) = aT_n^4(\underline{r})$, and approximating the right side of the resulting equation implicitly, we get

$$\frac{U_r(\underline{r}, t) - aT_n^4(\underline{r})}{\beta_n} = (t - t_n) \sigma_n \left[\int_{4\pi} \psi(\underline{r}, \underline{\Omega}, t) d\Omega - cU_r(\underline{r}, t) \right] . \quad (29)$$

Solving for $U_r(\underline{r}, t)$, we obtain for $t_n \leq t < t_{n+1}$:

$$U_r(\underline{r}, t) = \frac{aT_n^4(\underline{r}) + (t - t_n) \beta_n \sigma_n \int_{4\pi} \psi(\underline{r}, \underline{\Omega}', t) d\Omega'}{1 + (t - t_n) \beta_n \sigma_n c} . \quad (30)$$

As desired, this expresses U_r in terms of ψ . Eq. (30) could be directly introduced into Eqs. (25) and (26) to alter the coupling of these equations in the manner described above. However, the Fleck-Cummings method employs an additional simplification: the time-dependent term $(t - t_n)$ in Eq. (30) is replaced by the constant $\alpha \Delta t_n$, with $0.5 \leq \alpha \leq 1$. Eq. (30) becomes, for $t_n \leq t < t_{n+1}$:

$$U_r(\underline{r}, t) = \frac{aT_n^4(\underline{r}) + \alpha \Delta t_n \beta_n \sigma_n \int_{4\pi} \psi(\underline{r}, \underline{\Omega}', t) d\Omega'}{1 + \alpha c \Delta t_n \beta_n \sigma_n} . \quad (31)$$

Eq. (31) is certainly less accurate than Eq. (30); for example, Eq. (31) is not exact at $t = t_n$. Also, the computational simplifications obtained by using Eq. (31) are minor; in an analog situation, one could employ Eq. (30) with little extra computational cost. [In fact, Eqs. (30), (25), and (26) constitute a method that approximates the ‘‘AMC-Implicit’’ method of Martin and Brown, described in these proceedings (Martin, 2001).] However, the standard IMC method is based on Eq. (31) for U_r , so we will not discuss Eq. (30) further in this paper.

Introducing Eq. (31) into Eqs. (25) and (26), we obtain for $t_n \leq t < t_{n+1}$:

$$\frac{1}{c} \frac{\partial \psi}{\partial t} + \underline{\Omega} \cdot \underline{\nabla} \psi + (\sigma_{s,n} + \sigma_{a,n}) \psi = \frac{1}{4\pi} \left(\sigma_{s,n} \int_{4\pi} \psi d\Omega' + \sigma_{a,n} a c T_n^4 + q \right) , \quad (32)$$

$$\frac{\partial U_m}{\partial t} = \sigma_{a,n} \left(\int_{4\pi} \psi d\Omega' - acT_n^4 \right) , \quad (33)$$

with

$$\sigma_{s,n}(\underline{r}) \equiv \sigma_n(\underline{r}) \left(\frac{\alpha c \Delta t_n \beta_n(\underline{r}) \sigma_n(\underline{r})}{1 + \alpha c \Delta t_n \beta_n(\underline{r}) \sigma_n(\underline{r})} \right) , \quad (34)$$

$$\sigma_{a,n}(\underline{r}) \equiv \sigma_n(\underline{r}) \left(\frac{1}{1 + \alpha c \Delta t_n \beta_n(\underline{r}) \sigma_n(\underline{r})} \right) . \quad (35)$$

Eqs. (32) and (33) have the desired structure, and a simple Monte Carlo realization as well. Eq. (32) has the form of a conventional “neutron” transport equation, with scattering cross section $\sigma_{s,n}$ and absorption cross section $\sigma_{a,n}$. [The “scattering” in Eq. (32) is often called “pseudo-scattering.”] Photons are “born” from the emission source $\sigma_{a,n}acT_n^4$ and the inhomogeneous source q . They “pseudo-scatter” throughout the medium in the conventional neutron transport way until (i) the end of the time step, (ii) they leak out, or (iii) they are absorbed. The photons that are emitted by the material are, appropriately, a gain term in Eq. (32) and a loss term in Eq. (33); and the photons that are absorbed by the material are a loss term in Eq. (32) and a gain term in Eq. (33). After Eq. (32) is simulated in the time step, Eq. (33) is integrated over the time step and each spatial cell to determine $U_{m,n+1} = U_m(\underline{r}, T_{n+1})$ in each spatial cell. This result determines T_{n+1} in each spatial cell. One then proceeds to the next time step.

Integrating Eq. (32) over $\underline{\Omega}$ and adding the result to Eq. (33), one obtains the energy balance Eq. (18). Thus, the IMC method conserves energy. However, the IMC method does not treat the emission-absorption process exactly. Physical photons undergo potentially many emissions and absorptions during a large time step. An IMC photon born during the time step undergoes potentially many pseudo-scattering events, and then at most *one* absorption, when its energy is deposited in the material until (at least) the beginning of the next IMC time step. (Clearly, pseudo-scattering is an approximation to emission.)

A spatial truncation error also occurs. When an IMC particle is absorbed, its energy is deposited in the spatial cell in which the absorption occurs, and the identity of the absorbed photon is lost. At a later time, the energy of the photon is emitted at a random point in the spatial cell. The randomization of the point of emission is equivalent to an unphysical “conduction” of energy through the material. This also degrades the accuracy of IMC simulations.

4. SEMI-ANALOG MONTE CARLO (SMC)

In the SMC method, the IMC truncation errors described in the previous two paragraphs are eliminated: the absorption-emission process is treated correctly, and there is no unphysical conduction of energy. For linear grey radiative transfer problems, the only errors in an SMC simulation are statistical. For nonlinear problems, space-time truncation errors occur because the temperature-dependent opacity and other “data” must be approximated on a space-time grid. (The correct physical transport process is simulated, but with slightly incorrect data evaluated at the beginning of the time step.)

Like IMC, the SMC method employs Eqs. (25) and (26) exactly, and Eq. (15) approximately. Since $U_m = U_m(T)$ and $U_r = aT^4$, then U_r is a known function of U_m :

$$U_r = U_r(\underline{r}, U_m) . \quad (36)$$

For $t_n \leq t < t_{n+1}$, we employ the approximation:

$$U_r(\underline{r}, t) \approx \eta_n(\underline{r}) U_m(\underline{r}, t) , \quad (37)$$

where

$$\eta_n(\underline{r}) = \frac{U_{r,n}(\underline{r})}{U_{m,n}(\underline{r})} = \frac{U_r[\underline{r}, U_{m,n}(\underline{r})]}{U_{m,n}(\underline{r})} = \frac{aT^4(\underline{r}, t_n)}{U_m[\underline{r}, T(\underline{r}, t_n)]} . \quad (38)$$

[Eq. (37) is exact for $t = t_n$. Also, for linear problems, as defined by Eqs. (19) - (23), Eq. (37) is exact, with

$$\eta_n(\underline{r}) = \eta(\underline{r}) .] \quad (39)$$

Introducing Eq. (37) into Eqs. (25) and (26), we obtain the following linearized grey radiative transfer equations:

$$\frac{1}{c} \frac{\partial \psi}{\partial t} + \underline{\Omega} \cdot \underline{\nabla} \psi + \sigma_n \psi = \frac{\sigma_n c \eta_n}{4\pi} U_m + \frac{q}{4\pi} , \quad (40)$$

$$\frac{\partial U_m}{\partial t} + \sigma_n c \eta_n U_m = \sigma_n \int_{4\pi} \psi d\Omega' , \quad (41)$$

which hold for $t_n \leq t < t_{n+1}$. These equations have the same structure as the linear grey equations (22), (23). They can be viewed as a time-dependent neutron transport equation [Eq. (40)], with no scattering, and one delayed neutron precursor group [Eq. (41)]. Therefore, they permit the following simple Monte Carlo realization:

In Eq. (40), a Monte Carlo particle is “born,” either from the emission source $\sigma_n c \eta_n U_m$ or from the inhomogeneous source q . The particle travels with speed c a mean distance of σ_n^{-1} (sampled from an exponential distribution), where it undergoes a collision. At the collision site, the particle is absorbed and a precursor atom is created [Eq. (41)], which emits exactly one particle a mean time $(\sigma_n c \eta_n)^{-1}$ (sampled from an exponential distribution) later.

With no loss of fidelity, one can instead interpret the absorbed particle as being “held” motionless at the absorption site within the material for a random length of time, after which it is emitted. With this interpretation, particles never lose their identity – each particle either streams from an emission site to an absorption site, or is absorbed motionlessly in the material, waiting to be emitted. Also, each particle is emitted at the same spatial point that it was earlier absorbed. (There is no unphysical conduction of heat or energy.) The sole distinction between absorption-emission and (real or pseudo-) scattering is:

- In a *pseudo-scattering* event, a particle is *immediately* released to stream on to its next collision site.
- In an *absorption-emission* event, an absorbed particle *waits* a certain delay time (sampled from an exponential distribution) to be released.

Thus, SMC particles – and energy – are preserved. An SMC particle either streams from a birth or emission site to its next absorption site (in which case its energy is assigned to the radiation), or it is absorbed in the material, waiting motionlessly to be emitted (in

which case its energy is assigned to the material). The *state* of a particle (streaming in the radiation, or absorbed in the material) determines whether its energy contributes to the radiation, or to the material. This simple bookkeeping procedure conserves the total (material + radiation) energy – until, of course, a particle leaks out of the system, taking its energy with it.

At the end of a time step, the value of the material energy density $U_{m,n+1}$ is obtained in each cell by determining the total number of particles “absorbed” in the cell, multiplying by the energy per particle, and dividing by the volume of the cell. Then, using the following exact relationship between $U_{m,n+1}$ and T_{n+1} [obtained from Eq. (11)]:

$$U_{m,n+1} = \int_0^{T_{n+1}} c_v(T') dT' , \quad (42)$$

we determine the temperature T_{n+1} in the cell at the beginning of the next time step. This enables one to re-evaluate the opacities and heat capacity at the new temperature, and to advance into the next time step.

The SMC method can easily include photon scattering. If scattering occurs, then when a streaming particle undergoes a collision event, a random number is drawn to decide whether the event is a scattering or an absorption. If the event is a scattering, the particle’s direction of flight changes into a random scattered direction of flight and the particle immediately streams toward its next random collision site. If the event is an absorption, then - as explained above - the photon is absorbed motionlessly in the material until a random emission time (sampled from an exponential distribution), when it is emitted in a random direction of flight.

The SMC Monte Carlo process faithfully represents the streaming, scattering, absorption, and emission processes. The only (truncation) errors occur because σ and η , which are generally nonlinear functions of T , and hence of U_m , are approximated on a space-time grid. If σ and η are independent of U_m , then the SMC Monte Carlo scheme is analog – it faithfully represents the radiative transfer physics, and the only errors in the simulation are statistical. Otherwise, the SMC method is not analog; the basic emission-absorption process is rendered faithfully, but σ and η are evaluated at the beginning of the time step, rather than evolving continuously in time in concert with the solution.

If Monte Carlo were applied to a time-dependent neutron transport process with delayed neutron precursors, and with temperature-dependent cross sections, this same nonlinear difficulty would occur. It would be necessary to evaluate the time- and space-dependent temperature on a space-time grid, and the temperature-dependent neutron cross sections would be evaluated (approximately) on the same grid. Because of this approximation, space-time truncation errors would occur, and the resulting Monte Carlo simulation would not be analog. (But, following our definition, it would be *semi-analog*.)

Finally, the SMC method proposed in this paper employs the simple approximation defined by Eqs. (37) and (38) to relate U_r and U_m . However, other more accurate linear relationships are possible. For example, one could use the first-order Taylor expansion:

$$\begin{aligned}
U_r &\approx U_r(\underline{r}, U_{m,n}) + \frac{\partial U_r}{\partial U_m}(\underline{r}, U_{m,n})(U_m - U_{m,n}) \\
&= U_r(\underline{r}, U_{m,n}) + \frac{\frac{\partial U_r}{\partial T}(\underline{r}, U_{m,n})}{\frac{\partial U_m}{\partial T}(\underline{r}, U_{m,n})}(U_m - U_{m,n}) \\
&= aT_n^4(\underline{r}) + \frac{4aT_n^3(\underline{r})}{c_{v,n}(\underline{r})}(U_m - U_{m,n}) \\
&= \left\{ aT_n^4(\underline{r}) - \frac{4aT_n^3(\underline{r})}{c_{v,n}(\underline{r})}U_{m,n} \right\} + \left\{ \frac{4aT_n^3(\underline{r})}{c_{v,n}(\underline{r})} \right\} U_m \\
&= \gamma_n(\underline{r}) + \beta_n(\underline{r})U_m .
\end{aligned} \tag{43}$$

Introducing Eq. (43) into Eqs. (25) and (26), we obtain

$$\frac{1}{c} \frac{\partial \Psi}{\partial t} + \underline{\Omega} \cdot \underline{\nabla} \Psi + \sigma_n \Psi = \frac{\sigma_n}{4\pi} (\gamma_n + \beta_n U_m) + \frac{q}{4\pi} , \tag{44}$$

$$\frac{\partial U_m}{\partial t} + \sigma_n (\gamma_n + \beta_n U_m) = \sigma_n \int_{4\pi} \Psi d\Omega' . \tag{45}$$

These equations have the same form as Eqs. (40) and (41), except for the inclusion of the γ_n terms. For linear problems as defined by Eqs. (19) and (20), $\gamma_n(\underline{r}) = 0$. Because of the γ_n terms and their ambiguous sign, a Monte Carlo realization of Eqs. (44) and (45) is more complicated than of Eqs. (40) and (41). For example, if $\gamma_n(\underline{r}) > 0$, then a certain component of the material energy at \underline{r} flows at a constant rate (during the time step) to the radiation. (This has the effect of altering the emission rate from the material.) A similar phenomenon occurs if $\gamma_n(\underline{r}) < 0$. We will not discuss Eqs. (44) and (45), or other possibilities, further in this paper.

5. NUMERICAL COMPARISONS

Here we compare the IMC and SMC methods for a grey, linear, 1-D radiative transfer problem solved previously by Su and Olson using a Fourier Transform (Su, 1997). The problem consists of Eqs. (22) and (23) defined on a homogeneous, infinite medium, with $c = \sigma = \beta = 1.0$, a zero initial condition at the initial time $t = 0.0$, and the 1-D source defined by $q(z, t) = 1.0$ for $|z| \leq 0.5$, and $0 \leq t \leq 10$, and $q(z, t) = 0.0$ otherwise. [Here z and t respectively have units of mean free paths (*mfp*) and mean free times (*mft*).] Thus, in a medium that is initially empty of photons, a histogram source 1.0 mfp wide is turned on for 10.0 mft. While the source is on, the photon population builds up near the source region and begins to “diffuse” away from it. After 10.0 mft, the source is turned off; the photon population then starts to fall near the source region, while continuing to “diffuse” away from it. The results shown in Figures 1-5 are based on IMC and SMC simulations, each using 10^6 source particles.

In Figure 1, the material energy density is plotted for $t = 1.0, 10.0,$ and 31.6 mft, for the Su-Olson, SMC, and IMC solutions – the latter obtained using $\alpha = 0.5$ with the “fine” space-time grid $\Delta z = 0.1, \Delta t = 0.1$. For these and all the figures shown in this paper, the Su-Olson and SMC solutions are identical, except for minor statistical errors. For the stated values of $\alpha, \Delta z,$ and $\Delta t,$ the IMC solution is virtually exact.

In Figure 2, the same problem is run again with $\alpha = 0.5$ and $\Delta t = 0.1,$ but with a “coarse” spatial grid: the region $|z| < 1$ enclosing the source has $\Delta z = 0.25,$ and the regions

to the left and right have $\Delta z = 2.0$. The IMC solution is accurate for $t = 1.0$, but slightly low in the source region and slightly high for large z for $t = 10.0$. This trend becomes more pronounced for $t = 31.6$. These observed IMC errors are consistent with spatial truncation errors, as discussed in the final paragraph of Section 3 above. (The relatively coarse spatial grid creates an artificial conduction of energy, which causes the energy to “diffuse” away from the source unphysically fast.)

Figure 3 displays the same problem as Figure 1, with $\alpha = 0.5$ and $\Delta z = 0.1$, but with a “coarse” time grid: $\Delta t_1 = 1.0, \Delta t_2 = 9.0, \Delta t_3 = \Delta t_4 = 10.0, \Delta t_5 = 1.6$. The error in the IMC solution is now greater at the intermediate time $t = 10$ than at the early time $t = 1.0$ or the late time $t = 31.6$. The reason for this is not clear.

Figure 4 displays the same problem with $\alpha = 0.5$, but with the coarse spatial grid of Figure 2 and the coarse time grid of Figure 3. The IMC errors in Figures 2 and 3 are (roughly) combined, as expected.

Figure 5 shows the same problem, with the same coarse space-time grid of Figure 4, but with $\alpha = 1.0$. The choice $\alpha = 0.5$ used in Figures 1 - 4 typically gives more accurate results for small Δt (Martin, 2001), but for coarser Δt , this value may not be optimal. In Figures 4 and 5, for $t = 1.0$, the $\alpha = 0.5$ solution (U_m) is clearly more accurate than the $\alpha = 1.0$ solution. For $t = 10.0$, the $\alpha = 0.5$ and $\alpha = 1.0$ solutions are comparably inaccurate, the former solution being much too high and the latter solution being much too low. For $t = 31.6$, the $\alpha = 1.0$ solution seems to be slightly more accurate than the $\alpha = 0.5$ solution.

Eqs. (34) and (35) show that when α increases, $\sigma_{s,n}$ increases and $\sigma_{a,n}$ decreases. This increases the distance that IMC particles travel between absorptions and decreases the rates at which the IMC particles are absorbed and emitted. Thus, at least for short times, IMC census particles should diffuse away from their point of origin more rapidly with $\alpha = 1.0$ than with $\alpha = 0.5$. This behavior is confirmed by the $t = 1.0$ and $t = 10.0$ plots in Figures 4 and 5.

In any event, it is clear that α is a “knob” (parameter) that must be selected by the user, based on experience and intuition. For coarse space-time grids, the value of α has an appreciable effect on the IMC solution, at least for intermediate times.

The numerical results cited above demonstrate the space-time truncation errors that occur in IMC solutions. The physical problem considered here is simple and only somewhat representative of practical problems, but it is one of the few nontrivial radiative transfer problems for which benchmark results exist. At this time, we cannot present numerical results for grey nonlinear problems. However, in our future work, testing the SMC method for nonlinear problems and comparing the results to IMC is a priority.

6. DISCUSSION

In this paper we have derived and tested a new “Semi-Analog Monte Carlo” (SMC) method for the simulation of grey radiative transfer problems. The SMC method eliminates some of the temporal and spatial discretization errors that occur in nonlinear IMC simulations. For linear grey radiative transfer problems, the SMC method is analog – the only SMC errors are statistical and limit to zero as $1/\sqrt{N}$, with N the number of histories. For nonlinear radiative transfer problems, the coefficients in the radiative transfer equa-

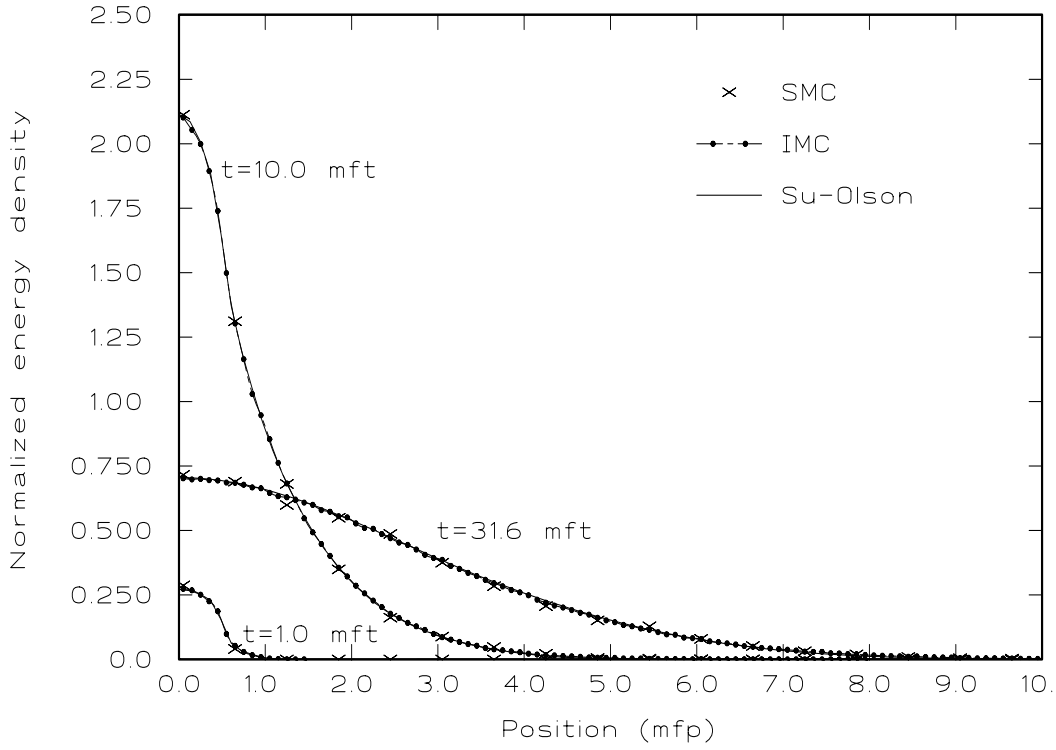


Fig 1: Material Energy Density ($\alpha = 0.5$, fine Δz , fine Δt)

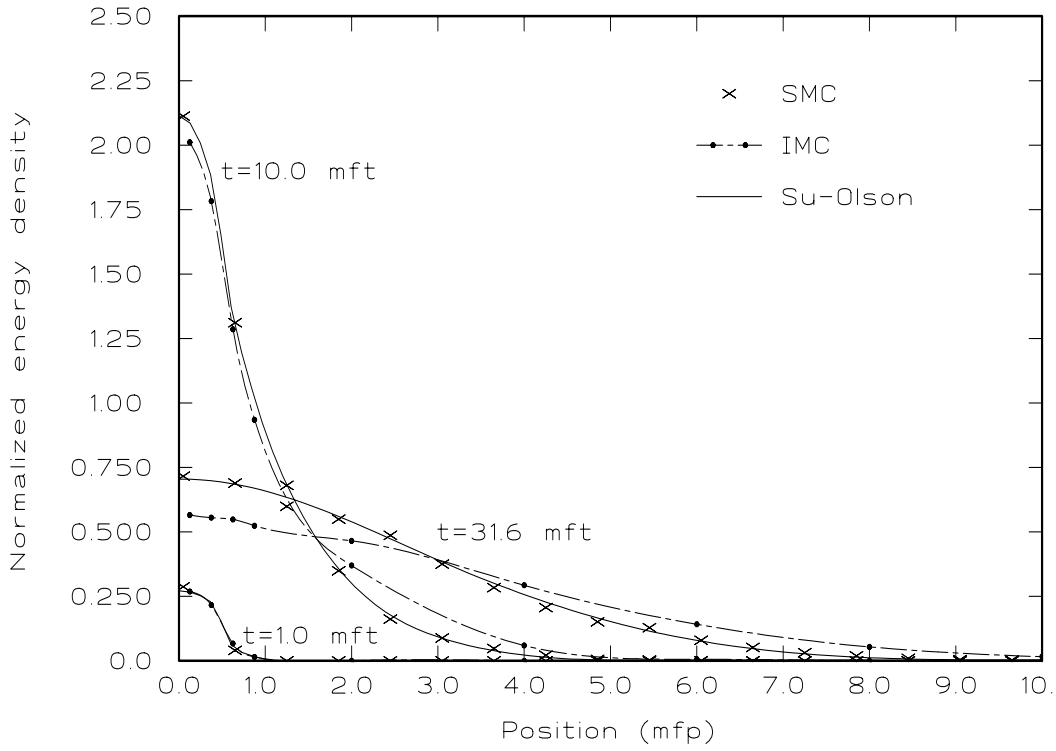


Fig 2: Material Energy Density ($\alpha = 0.5$, coarse Δz , fine Δt)

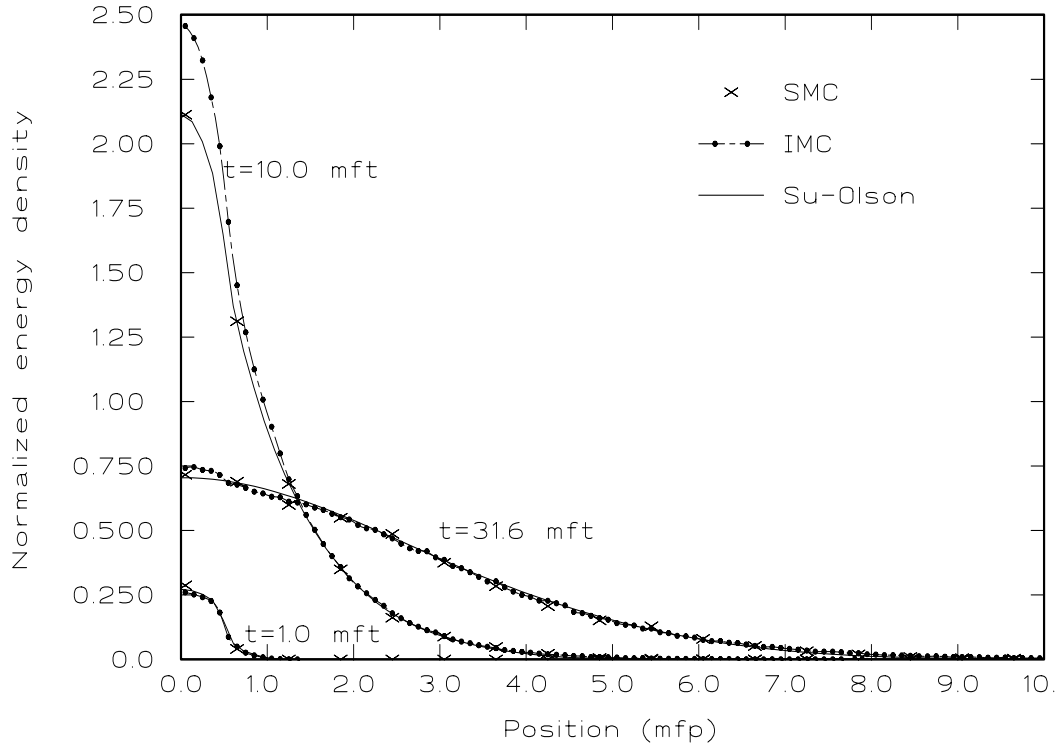


Fig 3: Material Energy Density ($\alpha = 0.5$, fine Δz , coarse Δt)

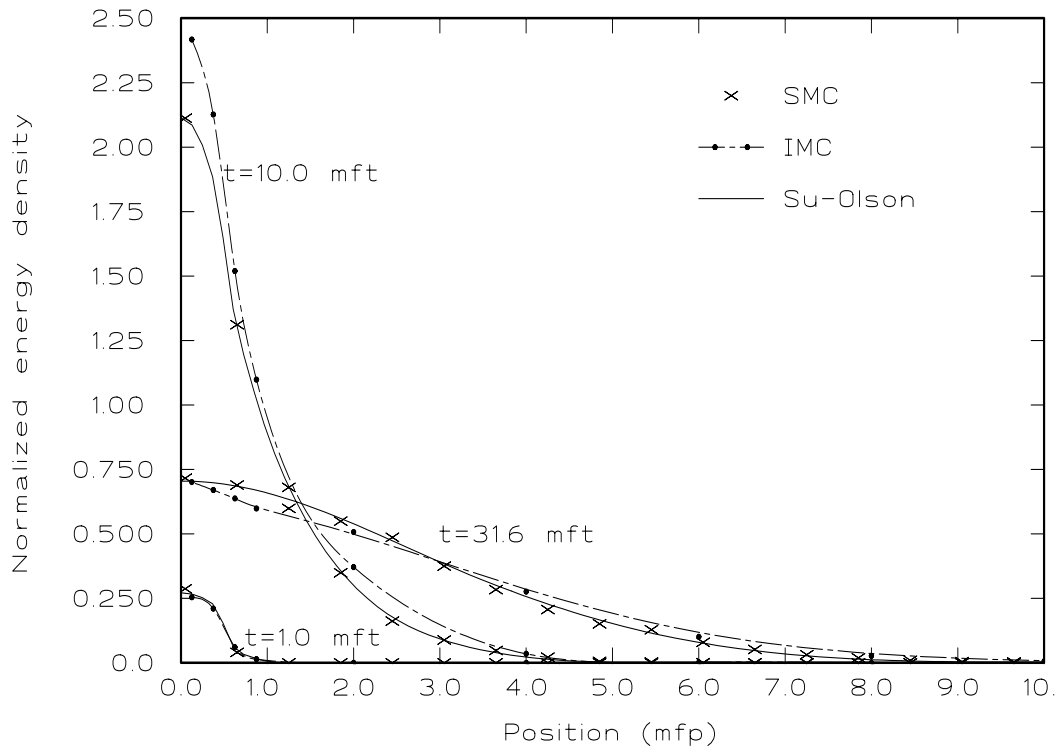


Fig 4: Material Energy Density ($\alpha = 0.5$, coarse Δz , coarse Δt)

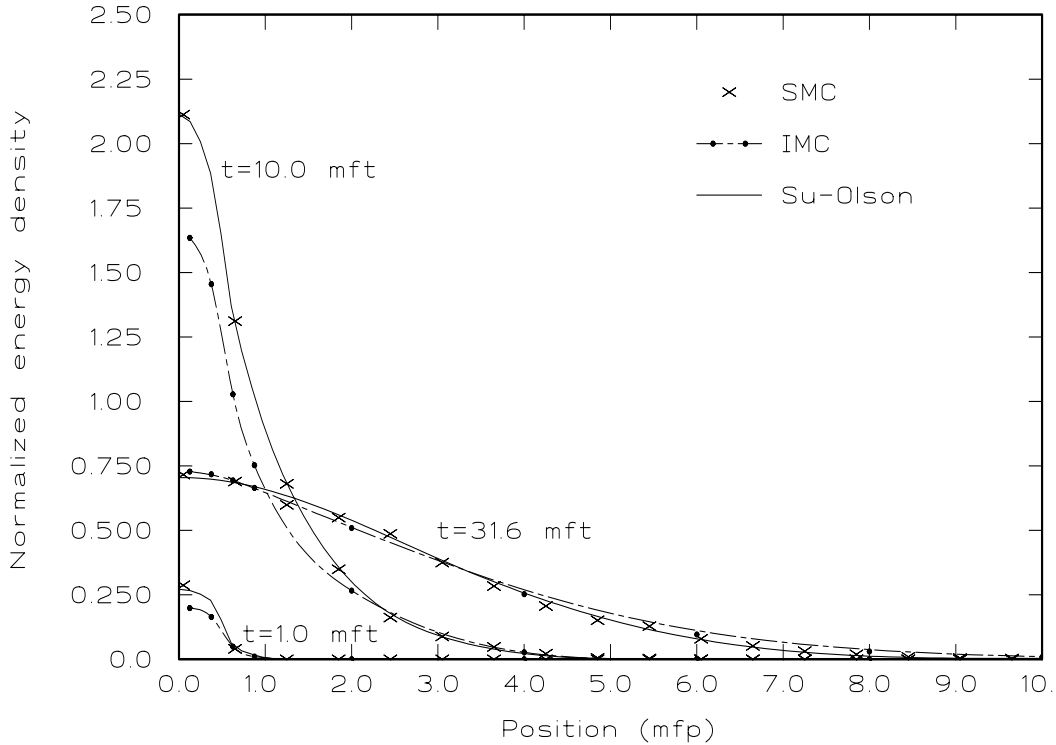


Fig 5: Material energy density ($\alpha = 1.0$, coarse Δz , coarse Δt)

tions depend on the material temperature, i.e. on the solution of the problem. In each time step, the space and time-dependence of these coefficients must be approximated, so the SMC method is no longer analog. (The same difficulties occur in time and temperature-dependent neutron transport problems with temperature-dependent cross sections.) The IMC method is never analog.

The IMC and SMC methods both conserve energy. However, the SMC method models the emission-absorption physics faithfully (IMC does not), the SMC method is significantly easier to implement, and numerical results demonstrate that for linear problems, the SMC method is more accurate.

In future work, we plan to (i) extend, implement, and test the SMC Monte Carlo method for nonlinear, multidimensional, frequency-dependent radiative transfer problems, and (ii) investigate more accurate SMC approximations, such as the one suggested by Eqs. (44) and (45).

ACKNOWLEDGMENTS

We gratefully acknowledge the helpful advice provided by Todd Urbatsch, Forrest Brown, and Bill Martin during the execution and writing of this work. This research was supported by the Los Alamos National Laboratory, under subcontract F02830018-2G.

REFERENCES

Ahrens, C. and Larsen, E.W., 2000. "An Exact Monte Carlo Method for Linear Grey Radiative Transfer Problems," *Trans. Am. Nucl. Soc.* **83**, 340-341.

Alcouffe, R.E., Clark, B.A., and Larsen, E.W., 1985. "The Diffusion-Synthetic Acceleration of Transport Iterations, with Application to a Radiation Hydrodynamics Problem," in *Multiple Time Scales*, J.U. Brackbill and B.I. Cohen (editors), Academic Press, New York, pp. 73-111.

Carter, L.L. and Forest, C.A. "Nonlinear Radiation Transport Simulation with an Implicit Monte Carlo Method," Los Alamos Scientific Laboratory Report, LA-5038, January, 1973.

Chester, C.R., 1971. *Techniques in Partial Differential Equations*, McGraw-Hill, New York, p. 8.

Fleck, J.A. and Cummings, J.D., 1971. "An Implicit Monte Carlo Scheme for Calculating Time and Frequency Dependent Nonlinear Radiation Transport," *J. Comp. Phys.* **8**, 313-342.

Larsen, E.W. and Mercier, B., 1987. "Analysis of a Monte Carlo Method for Nonlinear Radiative Transfer," *J. Comp. Phys.* **71**, 50-64.

Martin, W.R. and Brown, F.B., 2001. "Comparison of Monte Carlo Methods for Nonlinear Radiation Transport," Proc. ANS Topical Meeting: *International Conference on Mathematical Methods to Nuclear Applications*, September 9-13, 2001, Salt Lake City, Utah, submitted.

Mihalas, D. and Mihalas, B.W., 1984. *Foundations of Radiation Hydrodynamics*, Pergamon Press, Oxford.

Pomraning, G.C., 1973. *The Equations of Radiation Hydrodynamics*, Pergamon Press, Oxford, pp. 157-182.

Su, B. and Olson, G.L., 1997. "An Analytical Benchmark for Non-Equilibrium Radiative Transfer in an Isotropically Scattering Medium," *Ann. Nucl. Energy* **24**, 1035-1055.